Patient-Specific Liver Vasculature Phantoms for Y-90 Radioembolization Dosimetry

R. J. Dawson,[1,2] M. Bobić,[2] C. Beekman,[2] R. Atta,[2] E. Wehrenberg-Klee,[2] H. Paganetti,[2] W. E. Bolch,[3] A. Bertolet,[2] C. Huesa-Berral[2]

[1]*Medical Physics Program, University of Florida, Gainesville, FL* • [2]*Massachusetts General Hospital & Harvard Medical School, Boston, MA* • [3]*J. Crayton Pruitt Family Dept. of Biomedical Engineering, University of Florida*

Introduction

Transarterial radioembolization (TARE) with yttrium-90 (^{90}Y) microspheres exploits the differential perfusion of hepatocellular carcinoma (HCC)—fed mainly by the hepatic artery—versus normal parenchyma supplied by the portal vein. Microspheres lodge at ~100 µm arteriovenous junctions, so sub-resolution vascular architecture governs the spatial dose. Yet standard dosimetry assumes a homogeneous microsphere distribution and reports only mean absorbed dose (AD), ignoring the patient-specific vasculature behind the heterogeneity seen on post-treatment imaging. We reproduce and augment patient-specific hepatic vascular trees from cone-beam CT angiography (CBCT-A)—extending vessels beyond the imaging limit—to quantify how vascular heterogeneity shapes ^{90}Y dose.

Materials and Methods

Proof-of-concept: a right-lobe HCC patient treated with TARE.

1. Arterial segmentation — major hepatic arteries from CBCT-A via multiscale Hessian vesselness (ITK); automated mesh repair; VMTK centerlines.

2. Reference registration — sex-specific 8-segment Couinaud liver deformably registered (ANTs SyN) to the patient contour (Dice 0.98 liver, 0.99 PTA).

3. Territory partition — segmentation endpoints seed a 3-D Voronoi partition of the perfused target area (PTA).

4. Vessel extension — Murray's-law space-filling growth within each cell, down to ~100 µm terminal radii.

5. Heterogeneity α — reallocates a fixed endpoint budget between radius-weighted (α=1, heterogeneous) and volume-weighted (α=0, homogeneous) limits; six variants plus a synthetic baseline.

6. Dose & calibration — 2.5 GBq ^{90}Y at endpoints (tumor TNR 2.17) → synthetic SPECT → PHITS Monte Carlo (10^7 histories); α calibrated to [^{99m}Tc]Tc-MAA SPECT via 3-D gamma (10%/10 mm).

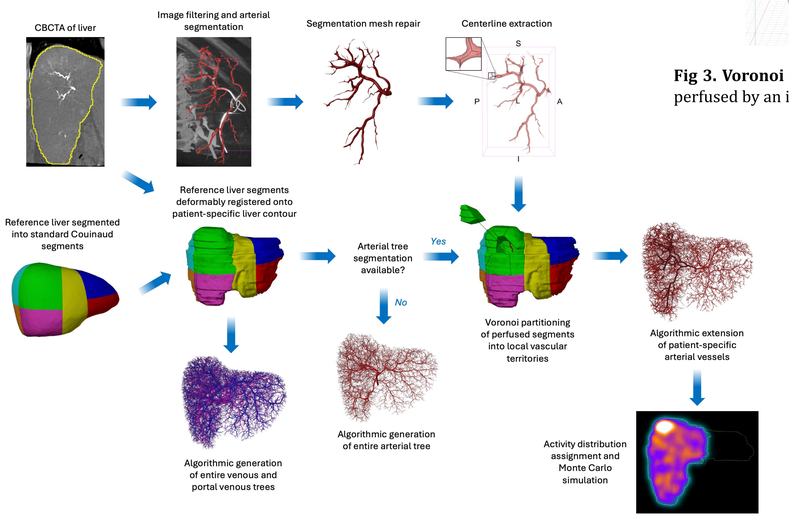

Fig 1. Modeling pipeline. CBCT-A arterial segmentation & mesh repair; deformable registration of an 8-segment Couinaud reference liver; Voronoi partition of the perfused target; Murray's-law vessel extension to ~100 µm; activity assignment & Monte Carlo dosimetry.

Results

Distinct vascular architectures produced very different dose heterogeneity despite identical mean AD. Mean dose was stable across all α (PTA 67–69 Gy; tumor 187–198 Gy). Heterogeneity concentrated in the high-dose tail: PTA D2 fell from ~450 Gy (α=1) to ~200 Gy (α=0), and the voxel maximum from 3.56×10^3 to 6.80×10^2 Gy; the tumor trend was larger (D2 ~700→~350 Gy). Relative to the synthetic baseline, the dose coefficient-of-variation (CV) ratio decreased monotonically with α—up to 5.1× (normal tissue) and 2.1× (tumor) at α=1—confirming that patient-specific geometry, not mean dose, drives non-uniformity.

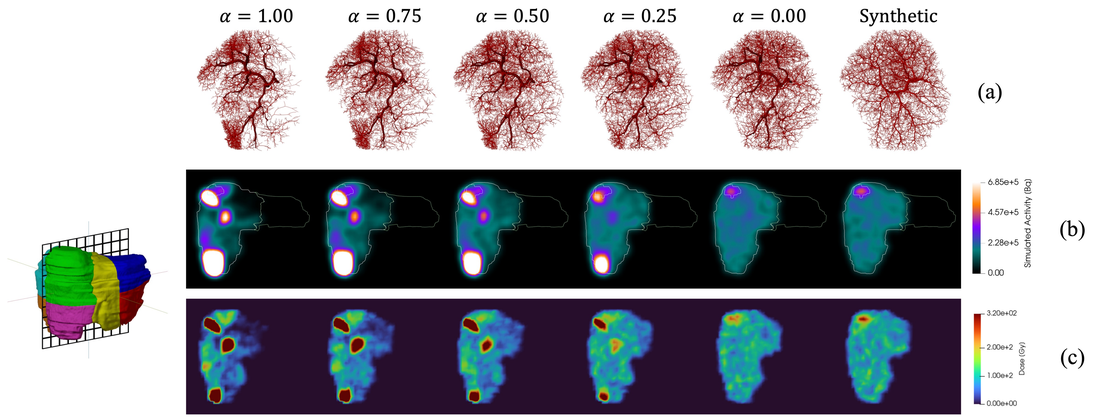

Fig 2. Effect of heterogeneity α. (a) vascular architecture, (b) synthetic SPECT activity, (c) ^{90}Y dose. α=1 clusters endpoints near large arteries (focal hotspots); α→0 gives uniform perfusion and homogeneous dose, matching the synthetic baseline.

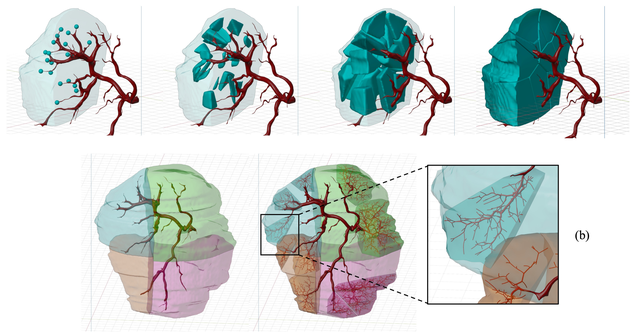

Fig 3. Voronoi territories. Segmentation endpoints seed Voronoi cells; each is perfused by an independent distal tree grown within its boundary.

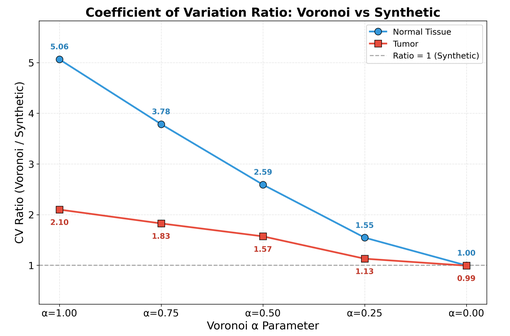

Fig 4. CV ratio (model ÷ synthetic) vs. α. Maximal heterogeneity (α=1) amplifies dose non-uniformity up to 5.1× (normal tissue) and 2.1× (tumor); ratios converge to 1 at α=0.

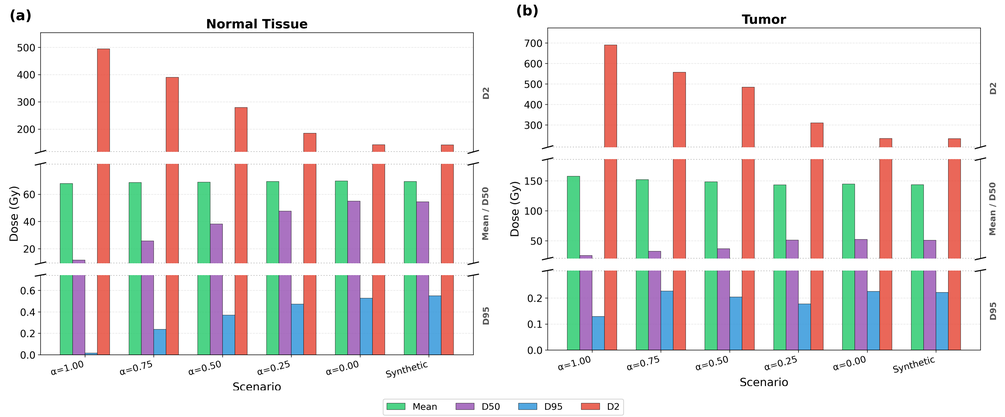

Fig 5. DVH metrics vs. α. Normal tissue (a) and tumor (b). Mean and D50 are stable; the high-dose tail (D2) falls monotonically as α decreases—isolating heterogeneity as the driver of dose non-uniformity.

Discussion

Patient-specific vasculature geometry directly modulates ^{90}Y dose heterogeneity even at fixed mean AD. Clinically this matters: focal hotspots may exceed normal-tissue tolerance while cold regions may permit recurrence—effects invisible to mean-dose planning. The framework is organ-agnostic (only the arterial anatomy is liver-specific) and couples directly to stochastic microsphere transport (MIDOS), Monte Carlo, and CFD, seeding calibratable digital twins. Because [^{99m}Tc]Tc-MAA and iodinated contrast differ hemodynamically, multi-phase CBCT-A is the preferred future calibration reference.

Model Calibration

Matching each model's synthetic [^{99m}Tc]Tc-MAA SPECT to the patient's clinical SPECT (3-D gamma, 10%/10 mm) gave a spline-interpolated optimal α = 0.41 and a maximum pass rate of 78.5%—showing that vascular heterogeneity can be calibrated from routine clinical imaging.

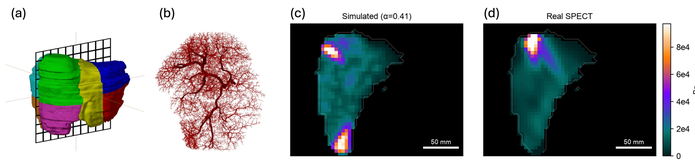

Fig 6. Calibration. Synthetic [^{99m}Tc]Tc-MAA activity at the fitted α=0.41 vs. the patient's clinical SPECT (same colour scale); 3-D gamma pass rate 78.5%.

Conclusion

Patient-specific vasculature geometry directly impacts ^{90}Y dose heterogeneity. This framework completes intrahepatic vascular trees from CBCT-A and provides a patient-specific way to study that effect—paving the way for calibratable digital twins and personalized TARE treatment planning.

Funding

NIH/NCI F31 CA288051, R01 CA248901, R00 CA267560, K99 CA312830; American Cancer Society PF-24-1317320-01-CTPS; SNMMI Student Research Grant. IRB: MGH 2014P001813.

Contact

Robert J. Dawson — rdawson@ufl.edu
Medical Physics Program, University of Florida

Advanced Laboratory for Radiation Dosimetry Studies